AGU PUBLICATIONS

JGR

Journal of Geophysical Research: Atmospheres

RESEARCH ARTICLE
10.1002/2013JD020696

Key Points:
- Extratropical-tropical interaction over the Indian Ocean during austral summer

Correspondence to:
Y. Fukutomi,
fukutomi@jamstec.go.jp

Citation:
Fukutomi, Y., and T. Yasunari (2014), Extratropical forcing of tropical wave disturbances along the Indian Ocean ITCZ, *J. Geophys. Res. Atmos.*, *119*, 1154–1171, doi:10.1002/2013JD020696.

Received 7 AUG 2013
Accepted 29 NOV 2013
Accepted article online 4 DEC 2013
Published online 6 FEB 2014

Extratropical forcing of tropical wave disturbances along the Indian Ocean ITCZ

Yoshiki Fukutomi[1] and Tetsuzo Yasunari[1,2]

[1]Research Institute for Global Change, Japan Agency for Marine-Earth Science and Technology, Yokohama, Japan, [2]Research Institute for Humanity and Nature, Kyoto, Japan

Abstract The role of extratropical waves in the excitation of tropical waves on submonthly timescales is explored along the Indian Ocean Intertropical Convergence Zone (ITCZ) during the austral summer using Japanese Reanalysis products and NOAA outgoing longwave radiation data. The analysis period is December–February of 1979/1980 to 2008/2009. The submonthly tropical waves are regarded as a type of Rossby wave propagating along the mean monsoon westerly flow. They play an important role in modulating the Indian Ocean ITCZ convection. The linkage between the tropical and extratropical waves, which is responsible for the formation and strengthening of tropical waves, is examined. Composite analysis results linked to the tropical wave train development show that the midlatitude Rossby wave train progresses eastward and northeastward from the South Atlantic into the subtropical Indian Ocean. As a trough and ridge that form part of the midlatitude wave train approach the southern Africa-southwest Indian Ocean (SWIO) region, a southwest-northeast-oriented wave train is subsequently established, originating from this feature, and is strengthened across the tropical Indian Ocean. The midlatitude wave propagation toward the subtropics induces the growth of the trough and ridge over the SWIO. Wave activity flux diagnostics indicate that the amplified trough and ridge over the SWIO act as an energy source for northeastward amplification of the tropical waves through the wave energy dispersion process. The results suggest that the propagation of the midlatitude wave toward the SWIO is the fundamental mechanism behind the development of the tropical waves along the Indian Ocean ITCZ.

1. Introduction

Low-level flow and convection along the Indian Ocean Intertropical Convergence Zone (ITCZ) are modulated by various space and timescale disturbances [e.g., *Krishnamurti et al.,* 1997; *Vincent et al.,* 1998; *Schrage et al.,* 2001; *Verver et al.,* 2001; *de Laat and Lelieveld,* 2002], such as the Atlantic and Pacific ITCZs. Overall location and strength of the Indian Ocean ITCZ change on the low-frequency (about 30–60 days) intraseasonal timescale due to the Madden-Julian Oscillation (MJO), while higher-frequency transient disturbances are responsible for local organization of convection within the ITCZ and its day-to-day fluctuation. Although the importance of high-frequency (about 6–30 days) intraseasonal and synoptic scale disturbances in the fluctuation of the Indian Ocean ITCZ has been widely recognized since the Indian Ocean Experiment [*Ramanathan et al.,* 2001], a smaller number of studies have considered a dynamic structure and development mechanism for high-frequency disturbances over the Indian Ocean ITCZ. The details, however, are poorly understood.

In this respect, *Fukutomi and Yasunari* [2013, hereinafter FY13] investigated the spatiotemporal structure and propagation characteristics of a dominant mode of wave disturbances on submonthly (high-frequency intraseasonal) timescales ranging from 6 to 30 days over the tropical Indian Ocean during the austral summer. They successfully identified the tropical wave train pattern oriented in a northeast-southwest direction from Sumatra toward Madagascar. The wave train exhibits westward-southwestward phase propagation and eastward-northeastward amplification, which could be due to wave energy dispersion across the Indian Ocean. The waves have a convectively coupled wave characteristic and play an important role in modulating the ITCZ convection. They discussed the dynamical nature of the waves and suggested that they can be regarded as a kind of Rossby wave mode propagating along the tropical waveguide produced by the mean monsoon westerly flow. Although they comprehensively documented the basic structure of the waves, the origin and initiation mechanism of the waves still remains uncertain. FY13 speculated that extratropical forcing is one possible excitation mechanism for the tropical wave development along the Indian Ocean ITCZ, and they stated that extratropical phenomena associated with the tropical wave development over the Indian Ocean are a subject of an extensive investigation.

Generally, extratropical-tropical interaction processes for exciting tropical disturbances along the ITCZ would be briefly categorized into two types as shown schematically by *Slingo* [1998]. One type is direct propagation of midlatitude waves toward the tropics. In oceanic regions, such as the Pacific, intrusion of a midlatitude wave train into the deep tropics initiates convectively coupled equatorial waves and modulates the ITCZ convection [e.g., *Kiladis et al.,* 1994; *Meehl et al.,* 1996; *Kiladis,* 1998; *Straub and Kiladis,* 2003]. The other effect consists of low-level meridional wind surges produced by midlatitude waves. As described by *Fukutomi and Yasunari* [2009], transient cross-equatorial flows induced by the meridional wind surges exert important lateral forcing on tropical disturbances, such as westerly wind bursts, convectively coupled equatorial waves, and tropical cyclones over the western Pacific [e.g., *Love*, 1985; *Chu*, 1988; *Kiladis et al.,* 1994; *Meehl et al.,* 1996; *Yu and Rienecker,* 1998; *Compo et al.,* 1999]. Various extratropical-tropical interaction phenomena over the Indian Ocean have also been reported previously, although by comparatively fewer studies. *Fukutomi and Yasunari* [2005, 2009] presented evidence that low-level southerly surges caused by Southern Hemisphere (SH) midlatitude wave propagation excite an equatorial convective disturbance over the eastern Indian Ocean during austral winter. *Fauchereau et al.* [2009], *Cretat et al.* [2012], and *Hart et al.* [2010] deduced that the northeastward propagation of midlatitude waves from the Atlantic toward the southwest Indian Ocean (SWIO) is linked to the development of tropical-temperate troughs (TTTs) during austral summer. A TTT is a northwest-southeast-oriented convective band coupled with an equatorward extended trough over southern Africa and the adjacent SWIO region [e.g., *Fauchereau et al.,* 2009; *Manhique et al.,* 2009; *Pohl et al.*, 2009; *Cretat et al.,* 2012; *Hart et al.,* 2010; *Vigaud et al.,* 2012] and is recognized as a heavy rainfall-producing system over southern Africa. *Davidson et al.* [2007] found that northeastward midlatitude wave propagation from the SWIO toward the Australian tropics can influence the onset of the Australian monsoon. Thus, various types of extratropical-tropical interaction linked to the predominant tropical variability have been found over the Indian Ocean. However, a series of previous studies on the TTT-related extratropical-tropical interaction has not noticed the linkage between the extratropical wave propagation and tropical wave development in the Indian Ocean ITCZ region.

As aforementioned, our previous study (FY13) found that the convective waves form the wave train propagating along the Indian Ocean ITCZ. Our next concern is whether and how extratropical waves are important for developing the tropical waves as identified by FY13. Hence, primary objective of this study is to detect a linkage between the tropical wave development and extratropical wave propagation over the Indian Ocean, and to determine a mechanism underlying that. We begin by identifying the primary wave mode along the Indian Ocean ITCZ using an extended empirical orthogonal function (EEOF) analysis. We then examine the spatiotemporal structure and evolution of the tropical waves using a composite analysis based on the EEOF analysis result, considering the relationship with the extratropical wave motions. The role of extratropical wave propagation on tropical wave development is discussed using dynamical diagnostics. Data for 30 winters (December–February) from 1979/1980 to 2008/2009 are analyzed. A brief description of the data sources and data processing procedure is presented in section 2. The results of the composite analysis highlighting the structure and evolution of tropical waves due to extratropical wave influences can be found in section 3. The dynamical diagnostics for the extratropical forcing of tropical waves is presented in section 4. Finally, a summary and discussion can be found in section 5.

2. Data Sets and Processing

The data used in this study are the Japanese 25 year Reanalysis (JRA25) and its extended version, the Japan Meteorological Agency (JMA) Climate Data Assimilation System (JCDAS) products, which have been produced through the JMA numerical assimilation and forecast system. The JRA25-JCDAS data set provides many kinds of assimilated and forecast variables available at a 6 h temporal resolution on various grid types [*Onogi et al.,* 2005, 2007]. We extracted the atmospheric horizontal winds, geopotential height, and temperature on a 2.5° grid at 12 pressure levels (100, 150, 200, 250, 300, 400, 500, 600, 700, 850, 925, and 1000 hPa) from the "anl-p25" subset of the JRA25-JCDAS data set [see *Onogi et al.,* 2007]. We computed the stream function and relative vorticity from the horizontal winds using a spherical harmonic transform method. All the elements were daily averaged for data analysis. We also used daily outgoing longwave radiation (OLR) data as a proxy for convective activity. The OLR data were obtained from the Earth System Research Laboratory of the United States National Oceanic and Atmospheric Administration (NOAA).

The data analysis was carried out for 30 SH summers (December–February: DJF) from 1979/1980 to 2008/2009. Prior to the data analysis, the annual mean and the annual cycle were removed from the original

365 day time series to extract subseasonal anomalies. The annual cycle is determined by calculating a sum of the first three harmonics of the original time series. The subseasonal anomalies were then passed through a 6–30 day band-pass filter to isolate submonthly scale fluctuations using the Butterworth filtering procedure of *Kaylor* [1977], following FY13. The filtered anomalies were used in the EEOF and composite analysis in the later sections.

3. Structure and Evolution of the Tropical Waves Associated With the Midlatitude Wave Propagation

3.1. EEOF Analysis

An EEOF analysis was applied to the filtered 850 hPa meridional wind to determine the primary modes of tropical waves over the tropical Indian Ocean. EEOF analysis has been widely used for extracting propagating wave modes in the tropics [e.g., *Lau and Lau*, 1990; *Maloney and Dickinson*, 2003]. FY13 successfully identified the dominant wave modes over the tropical Indian Ocean. The procedure used was essentially the same as that used in FY13 except for the analysis domain and total data length. We used a domain enclosed by 22.5°S–12.5°N, 35°E–110°E to identify the same type of wave patterns as those identified by FY13 as being successive leading modes. We first constructed a lagged covariance matrix with two 1 day lags at −1, 0, and +1 days from the time series for each DJF at each grid point in the domain, and then solved an eigenvalue problem to isolate the leading modes. The resulting principal component (PC) time series in terms of time coefficients of the EEOF was used as an index to construct composite fields of the atmospheric variables in the latter sections. The resulting first two EEOFs are shown in Figure 1. EEOFs 1 and 2 explain 7.7% and 6.9% of the total variance, respectively. These patterns are similar to each other and show a quadrature phase shift, suggesting that EEOFs 1 and 2 constitute a pair of modes that represent the same propagating wave. It should be noted that pairs of two EEOFs at lag −1 and +1 days show a similar pattern and a phase relationship to those at lag 0 day (not shown). The PC time series are shown for DJF 2000/2001 (Figure 1c). PC 1 and PC 2 time series have similar temporal structures, with PC 2 leading PC 1 by a few days. Lag-correlation analysis indicates that PC 2 leads PC 1 by 2 days (at a lag of −2 days) with a maximum correlation coefficient of 0.68. Note also that the correlation coefficient indicates a still relative higher value of 0.66 at with a lag of −3 days. A power spectrum of the PC 1 time series was estimated using a Fast Fourier transform method in the same manner as *Fukutomi and Yasunari* [2013]. The resulting spectrum (Figure 1d) has large power at periods of roughly 10–20 days. The EEOF modes exhibit a southwest-northeast-oriented wave train, which extends from Madagascar toward Sumatra Island, and they are very similar to the EEOF patterns obtained by FY13. This suggests that the present EEOF analysis successfully identified the same type of westward and southwestward propagating wave modes detected by FY13. We additionally performed an EEOF analysis for four 1 day lags [e.g., *Vera et al.,* 2002] over the same domain. This test produced very similar patterns of two leading EEOFs (not shown) to those in Figures 1a and 1b. This suggests that changing lag size for the EEOF analysis does not affect the resulting patterns in the present case.

3.2. Composite Analysis Procedure

To examine spatial and temporal structure and evolution of the waves propagating over the Indian Ocean, we created composites of various atmospheric fields based on the EEOF analysis results. We employed the PC 1 time series as a single index to pick out temporal phases to create the composite fields. We selected both positive and negative peak events of the index whose values exceeded the 1.5 standard deviation criteria. As a result, 57 positive and 68 negative events were identified. The timing of the peak of the index is referred to as the *day 0* phase for the daily lagged composites. The composites constructed based on the positive and negative peak (day 0) phases are referred to as *positive composites* and *negative composites*, respectively.

3.3. Horizontal Structure

The basic structure and evolution of the submonthly scale ITCZ waves are presented based on the negative composites that contain a larger number of peak events. Figure 2 shows the composite evolution of the 6–30 day filtered 850 hPa meridional wind anomalies and wind vectors over the Indian Ocean region from a lag period of −4 days to +2 days, with a 2 day interval. A southwest-northeast-oriented wave train extends across the tropical and subtropical Indian Ocean throughout the sequence. Axes of anomalous troughs and ridges of the wave train are tilted in a northwest-southeast direction. By day −4, a ridge-trough-ridge-trough pattern extending from the SWIO to the eastern equatorial Indian Ocean is established. The troughs and

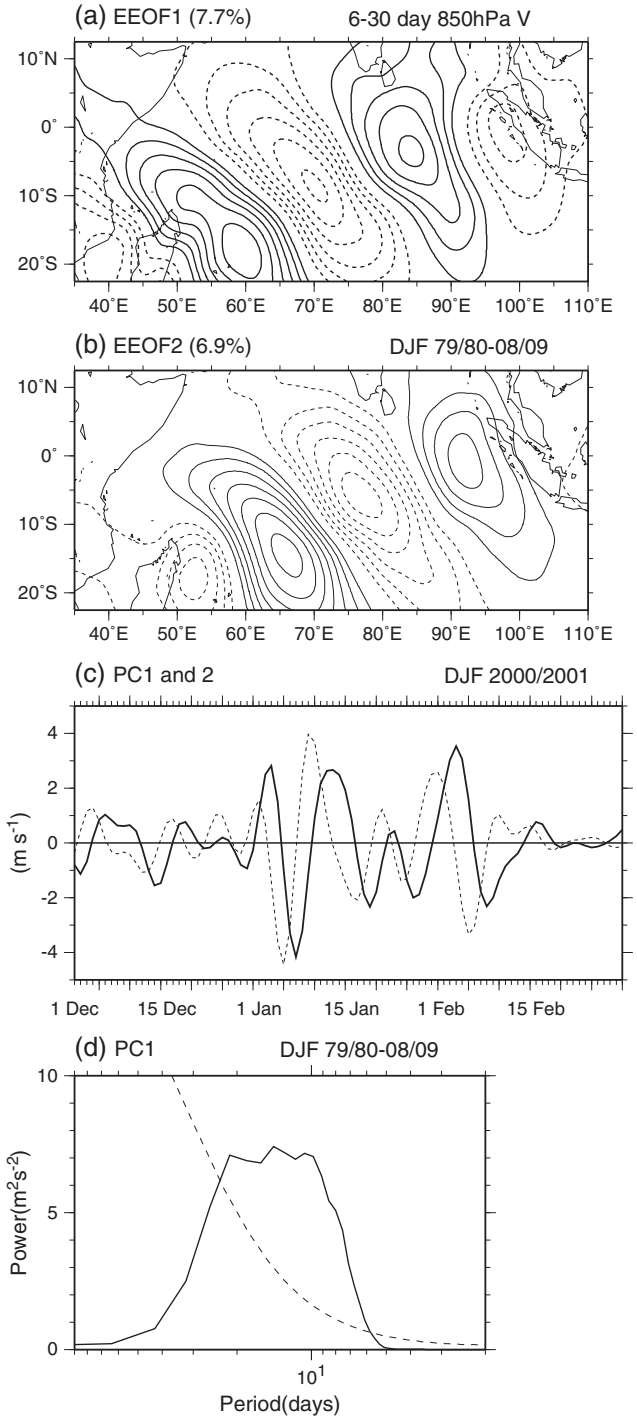

Figure 1. The leading two EEOFs of 6–30 day filtered 850 hPa meridional wind anomalies for DJF 1978/1979–2007/2008. (a) EEOF1 and (b) EEOF2. Contour interval is 0.1 (unit of correlation coefficient. Solid (dashed) contours indicate positive (negative) values. (c) PC 1 (solid line) and PC 2 (dashed line) for DJF 2000/2001. (d) Average power spectrum of PC 1 (solid line) and a 95% confidence limit (dashed line).

ridges (denoted by T and R) subsequently propagate westward and southwestward from the eastern equatorial region toward the southwest Indian Ocean region. From day −4 to day −2, the wave signals gradually grow as they propagate southwestward. At day 0, the waves are maximally amplified with an arc-like wave train structure extending from the southeast African coast across to the Island of Sumatra. At day +2, the waves continue to propagate and decay slightly. Overall, good qualitative agreement of the wave features

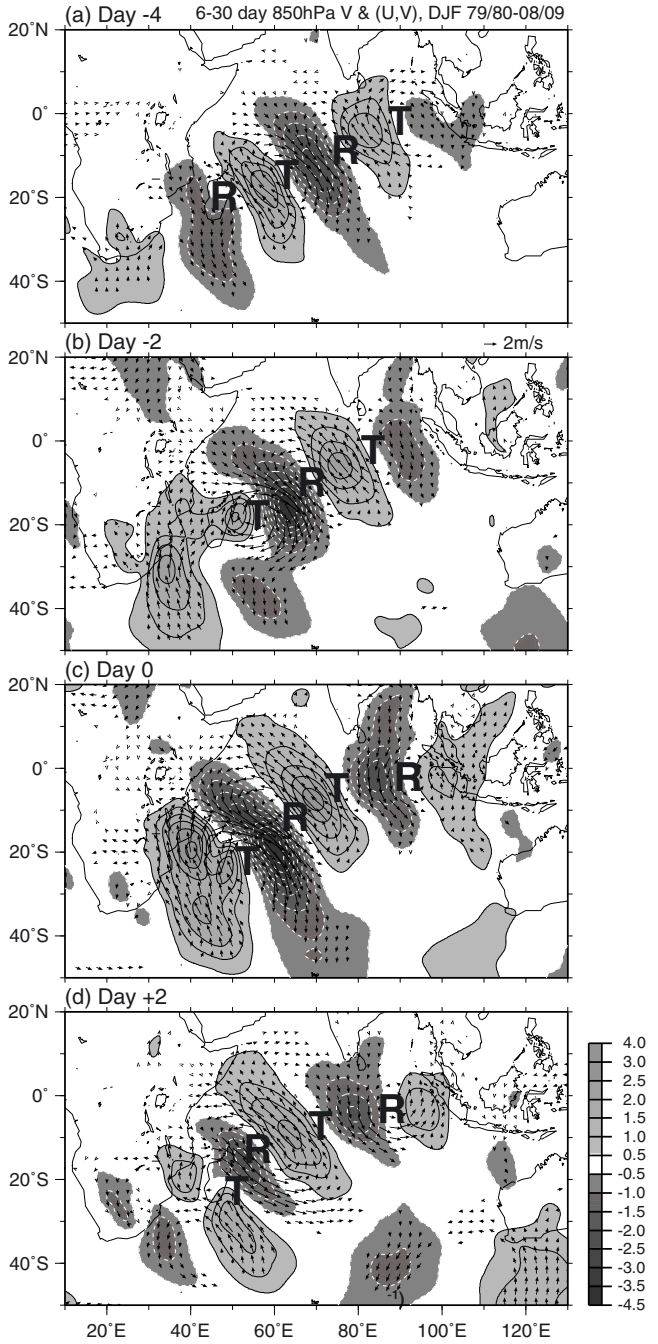

Figure 2. Lagged composites of 6–30 day filtered 850 hPa meridional wind anomalies (shades and contours) and wind vectors from day −4 through day +2 based on the PC1 index. Lighter shades with solid black contours (darker shades with dashed white contours) indicate positive (negative) values. Contour interval is 0.5 m s^{-1}. Zero contour is omitted. Locally statistically significant wind vectors at the 95% level are plotted. The T and R annotations refer to trough and ridge centers, respectively.

exists with those found by FY13. Note that the wave patterns in the positive composites of the same elements (not shown) are almost opposite to those in Figure 2.

To explore the relationship between tropical waves and SH extratropical systems, we consider composite wave evolution in both the lower and upper troposphere over a broad domain including the South Atlantic. Figure 3 shows a composite sequence of the 850 hPa stream function, wind vector, and OLR anomalies from day −6 to day +2. At day −6, weak gyre-type disturbances initially exist over the tropical Indian Ocean. A cyclonic (clockwise) circulation couples with the convective signal (negative OLR anomalies) in the ITCZ region. A wave train structure is not yet well organized at this stage. By day −4, an extratropical-tropical

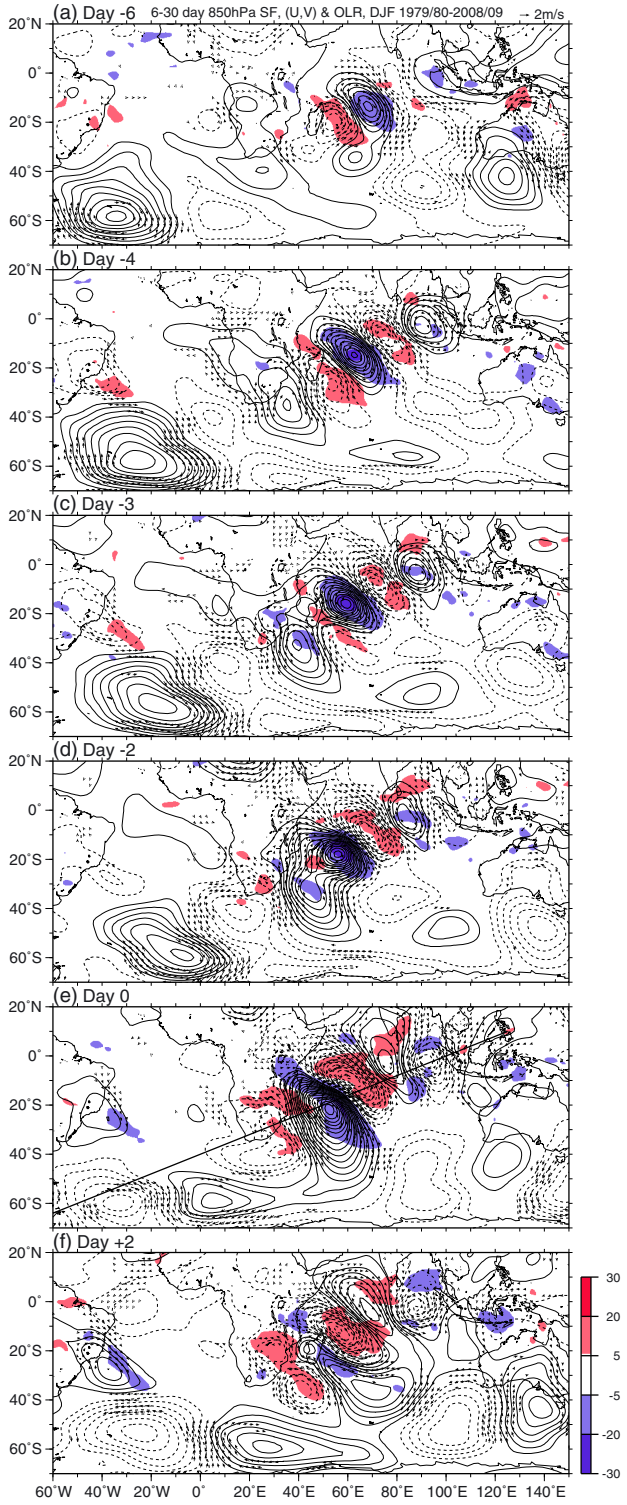

Figure 3. Lagged composites of 6–30 day filtered 850 hPa wind vectors, stream function, and OLR anomalies from day −6 through day +2 based on the PC1 index. Positive (negative) stream function contours are solid (dashed). Contour interval is 2.0×10^5 m^2 s^{-1}. Negative (positive) OLR anomalies are shaded with blue (red) colors. Locally statistically significant wind vectors at the 95% level are plotted. (e) The sick line extending northeastward from 62.5°W, 65°S to 125°E, 10°N is used for the vertical cross sections (Figure 5).

wave train traversing the subtropical and tropical Indian Ocean has been established involving the pre-existing disturbances. This southwest-northeast-oriented wave train seemingly originates from the South Atlantic region. The consecutive trough-ridge pattern spanning the South Atlantic to the eastern equatorial Indian Ocean is somewhat similar to that extending from the SWIO to the north of Australia identified by *Davidson et al.* [2007], although the present wave train axis (Figure 3b) is shifted westward about 50° from theirs. From day −4 to day +2, anomalous troughs and ridges constituting the wave train propagate westward and southwestward from the equatorial eastern Indian Ocean into the SWIO. However, the wave train exhibits northeastward amplification leading to the successive formation of new equatorial gyres over the eastern Indian Ocean. The northeastward-eastward amplification of the tropical waves could be due to dispersion of Rossby wave energy along the mean monsoon westerly flow as discussed by FY13.

Here a midlatitude trough-ridge couplet over the Southeast Atlantic-southern African region exhibits some interesting behavior. The couplet appears to constitute the extratropical-tropical wave train at day −4. While the tropical troughs and ridges of the wave train continue to travel westward and southwestward, the midlatiude trough-ridge couplet progresses eastward and northeastward. The northwest-southeastward oriented trough of the couplet extending from the SWIO to southern Africa at this time is similar as TTT [*Fauchereau et al.*, 2009; *Manhique et al.*, 2009; *Pohl et al.,* 2009; *Cretat et al.,* 2012; *Hart et al.,* 2010; *Vigaud et al.,* 2012]. This TTT-like trough moves northeastward while the tropical trough accompanying the convection moves southwestward from day −4 to day +2. They then merged into a single trough, which develops a northwest-southeastward tilt over the SWIO. This large-amplitude trough couples with a meridionally elongated convective band over the SWIO by day 0. This convective band extending from the SWIO into tropical eastern Africa is aligned with the northwesterly flow at the northeastern edge of the trough at day 0. This pronounced trough and convective band resemble a TTT and TTT cloud band over the southwest Indian Ocean, categorized as TTT regime 7 by *Fauchereau et al.* [2009]. At this stage, this TTT-like trough has reached full maturity and that then appears to induce further amplification of the waves toward the eastern Indian Ocean. Also note that the ridge located on the western side of the southern African TTT-like trough also moves eastward and eventually incorporates with the prevailing wave train over the subtropical and tropical Indian Ocean by day +2.

The low-level composite results discussed above imply that midlatitude wave propagation from the South Atlantic toward the SWIO is closely related to tropical wave development over the Indian Ocean. We next examine the upper-level circulations to gain a clear picture of the midlatitude wave propagation associated with the low-level wave development. Figure 4 displays the composite 200 hPa stream function and wind vector anomalies together with the DJF climatology of the meridional gradient of absolute vorticity $\beta - \overline{u}_{yy}$, where $\overline{u}$ is the DJF mean zonal wind, β is the meridional gradient of planetary vorticity, and $-\overline{u}_{yy}$ is the approximated meridional gradient of relative vorticity. $\beta - \overline{u}_{yy}$ is used to capture the wave guide nature of the midlatitude westerly region [e.g., *Hsu and Lin,* 1992]. Two split bands of the $\beta - \overline{u}_{yy}$ maximum take place over the Indian Ocean. One occurs along 50°S and is coincident with the midlatitude westerly jet during SH summer (not shown). The other lies along subtropical latitudes around 25°S. Throughout the evolution of the waves, individual wave centers tend to travel along both bands, suggesting that they could act as subtropical and midlatitude wave guides for the submonthly scale Rossby waves across the Indian Ocean. A composite sequence from day −6 to day +2 highlights the spatiotemporal evolution of upper-level extratropical Rossby waves with zonal wave numbers of 5–8 from the midlatitude South Atlantic into the subtropical Indian Ocean. At day −6, a short wave train appears over the subtropical Indian Ocean. By day −4, a wave train is established between the south of South Africa and Australia. The subtropical part of the wave train appears to link to the earlier growth of the low-level subtropical-tropical wave train (Figure 3b). From day −2 to day 0, a new wave-growing signals progresses eastward and northeastward from the midlatitude South Atlantic toward the subtropical Indian Ocean. At day 0, the waves fully develop to become a southwest-northeast-oriented wave train with downstream amplification, which could be produced by Rossby wave energy dispersion from the South Atlantic into the subtropical Indian Ocean. Troughs and ridges of the wave train are meridionally elongated and their axes are tilted in a southeast-northwest direction. They straddle both the subtropical and midlatitude wave guides over the SWIO. At this stage, the development of the upper-level wave train synchronizes with the northeastward amplification of the low-level waves (Figure 3d). In particular, the low-level TTT-like trough development over the SWIO is accompanied by the eastward evolution of a trough as part of the upper-level wave train. As the upper-level trough approaches the SWIO from the west, the corresponding low-level trough exhibits similar behavior. As

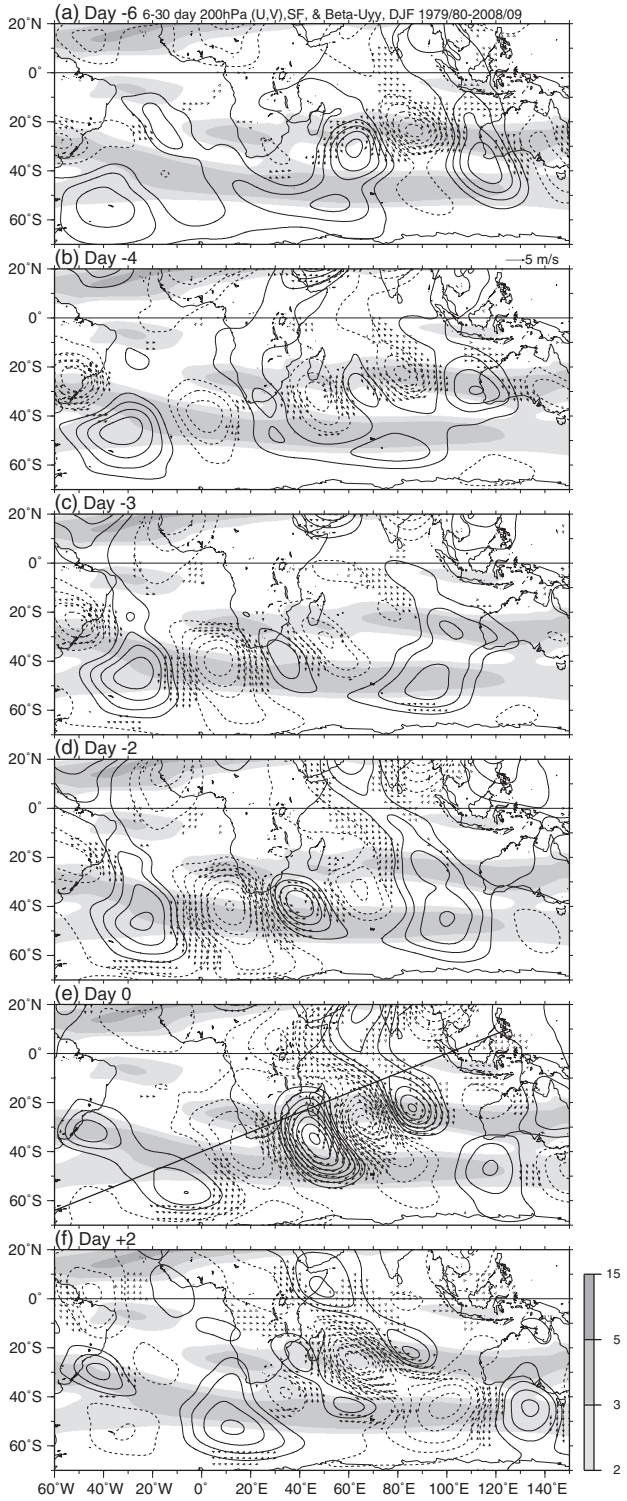

Figure 4. Lagged composites of 6–30 day filtered 200 hPa wind vectors and stream function anomalies from day −6 through day +2 based on the PC1 index. Shades represent 30-SH summer climatology of 200 hPa meridional gradient of absolute vorticity, starting at 2.0×10^{-5} s^{-1}. Contour interval for stream function is 5.0×10^{-5} s^{-1}. Locally statistically significant wind vectors at the 95% level are plotted. (e) The sick line extending northeastward from 62.5°W, 65°S to 125°E, 10°N is used for the vertical cross sections (Figure 5).

mentioned previously, this low-level trough develops as the TTT-like trough merges with the southwestward moving trough originating in the tropical wave train. When the upper-level trough arrives at the SWIO, the corresponding low-level trough axis is located to the northeast ahead of the upper-level trough axis, suggesting that baroclinic development of the convectively coupled trough occurs through the northeastward progression of the midlatitude waves.

Another noteworthy aspect of the upper-level waves is the separation of the wave train over the central Indian Ocean. From day −2 to day +2, the wave propagation path splits into two branches to the east of 60°E. One branch is the subtropical path, which is associated with the aforementioned low-level tropical wave development, and the other branch is the midlatitude path through which the waves propagate off the south coast of Australia. They almost overlap the bands of large meridional gradient of absolute vorticity, which are evidently favorable for guiding Rossby waves. The midlatitude path is consistent with the location of the midlatitude wave guide over the South Indian Ocean, as deduced by *Hsu and Lin* [1992]. The separation of the wave train appears to begin at day −2, and a clear dual wave train structure is completed by day +2. Whereas the subtropical waves exhibit westward phase propagation after their full development, the midlatitude waves continue to propagate eastward toward the Pacific. The retrogressive nature of the subtropical waves may be due to the comparatively weaker westerly basic state at latitudes of 20°–30°S.

Overall, the composite sequences show that the propagation of midlatitude waves plays an important role in the low-level tropical wave setup and amplification over the Indian Ocean. The midlatitude waves originating from the South Atlantic can propagate into the subtropical Indian Ocean and interact with low-level tropical waves extending into the equatorial eastern Indian Ocean. As the upper-level waves propagate northeastward into the subtropical Indian Ocean, they progressively strengthen through wave energy dispersion and form a southwest-northeast-oriented wave train. The upper-level trough over the SWIO strengthens as part of the wave train involves the development of the low-level trough accompanying the southeast-northwest-oriented convective band. These troughs exhibit baroclinic development that could be stimulated by the midlatitude wave propagation and energy dispersion process. One can expect that this trough development leads to amplification of the low-level tropical waves farther downstream through wave energy dispersion, along the monsoon westerly flow toward the equatorial eastern Indian Ocean.

3.4. Vertical Structure

We also examine the vertical structure of the wave train extending from the midlatitudes to the tropics, in a similar manner to the examination of the horizontal composites. Composite meridional wind anomalies at 12 pressure levels were produced along a southwest-northeast tilted line extending from 62.5°W, 65°S to 125°E, 10°N. This line approximately corresponds to the axis of the wave train in the low-level horizontal composites (Figure 3). Figure 5 displays vertical cross sections of the meridional wind anomalies from day −6 to day +2. This enables us to reveal the behavior of wave anomalies both in the tropics and extratropics, and the extent of the vertical coupling of the waves along the wave propagation path. Throughout the sequence, a well-developed train of deep northerlies and southerlies forms in the line. The meridional wind perturbations retain an equivalent barotropic vertical structure extending up to 300–400 hPa in the tropics to the east of 40°E. However, they tend to be slightly tilted in a southwestward direction at a height of 1000 to 200–150 hPa in the midlatitudes to the west of 40°E, implying weak baroclinic structure throughout the entire troposphere. Tropical wave signals continue to move southwestward between 40°E and 120°E, while midlatitude wave signals progress northeastward to the southwest of 40°E. The amplitude of the tropical signal tends to be larger in the lower troposphere while that of the midlatitude signal shows a maximum in the upper troposphere. At day −6, a train of weak tropical wind signals is isolated between 45°E and 90°E. By day −4, midlatitude signals begin to organize from the west while the tropical signals move southwestward. From day −2 to day 0, the tropical and midlatitude signals meet and merge into one around 40°E, which is consistent with the merging of the trough observed in the low-level composites (Figure 3). At day 0, a pronounced phase tilt with height occurs in the southwestward direction in the upper troposphere, suggesting the baroclinic development of the waves. From day −4 to day +2, wave amplification signals are transmitted toward the northeast in the middle and lower troposphere, and new perturbation cells sequentially appear around 100°E, indicating that wave energy dispersion toward the equatorial Indian Ocean occurs along the wave train axis.

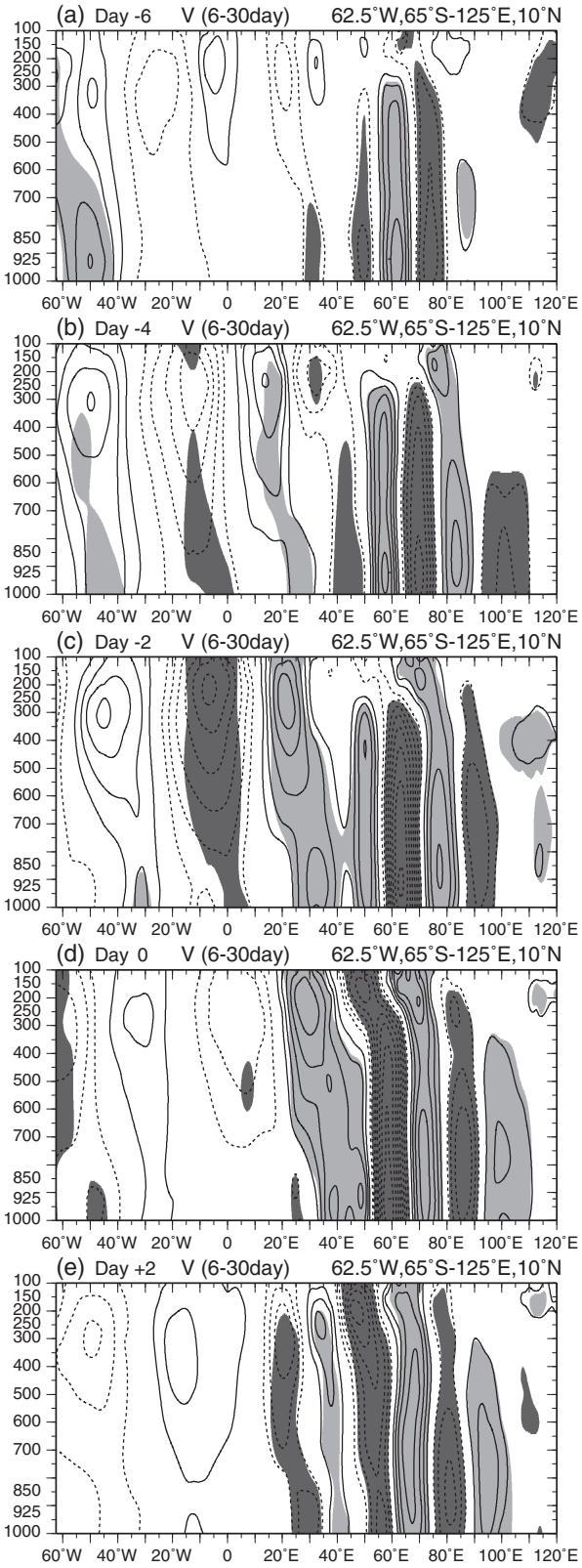

Figure 5. Vertical cross sections of meridional anomalies from day −6 through day +2 along the line extending from 62.5°W, 65°S to 125°E, 10°N (Figure 6c). Contour intervals is 0.5 m s^{-1}. Solid (dashed) contours indicate positive (negative) values. Positive (negative) anomalies with statistically significant at the 95% level are light (dark) shaded.

4. Wave Activity Diagnostics

The results of the composite analysis suggest that the midlatitude wave is an important factor leading to the development of the tropical wave train. The propagation of a midlatitude wave toward the subtropics could induce the growth of a trough and ridge over the SWIO. The amplified trough and ridge then appear to act as an initial energy source for northeastward development of the tropical waves through the wave energy dispersion. The wave activity flux (WAF) vector generalized by *Takaya and Nakamura* [1997, 2001] is used to show that wave energy dispersion is responsible for the composite results. We employed the two-dimensional (horizontal) formulation of the stationary component of the WAF. We used the perturbation geostrophic wind and geostrophic stream functions estimated from the composite geopotential height anomalies to compute the WAF. The wave packet was defined by an envelope function computed by a complex demodulation method [e.g., *Chang and Yu,* 1999; *Seager et al.,* 2010]. We computed the envelope function as the smoothed amplitude of the waves, which retained a zonal wave number for 0–15 components of the composite meridional wind anomalies. These tools give a clear picture of downstream amplification of the midlatitude waves propagating into the subtropics.

Figure 6 illustrates the evolution of the wave activity flux vectors together with wave packets at 200 hPa. The WAF vector and wave packet field are displayed for days −4, −2, and 0. At day −4, the WAF vectors are directed eastward and northeastward along an elongated wave packet extending from the midlatitude South Atlantic into the subtropical Indian Ocean, suggesting that downstream energy propagation promotes wave train formation along the upper-level subtropical wave guide (Figure 4b). This process could be relevant to the initial setup of the low-level tropical wave train with this timing (Figure 3b). Whereas the wave packet amplitude decreases over the subtropics, a new growing wave packet begins to progress from the South Atlantic toward the Indian Ocean, which accompanies enhanced wave energy propagation at day −2. By day 0, this wave packet signal proceeds northeastward into the subtropics and is amplified, corresponding to wave train development along the subtropical wave guide (Figure 4d). The WAFs are predominantly directed northeastward emanating from the south of southern Africa toward the eastern Indian Ocean throughout the wave packet. This wave packet amplification involves subtropical trough growth over the SWIO, which could facilitate the further development of low-level tropical waves such as those shown in the previous section. Here one notices that the strong WAFs are essentially embedded within the upper-level subtropical wave packet and do not penetrate deep into the tropics. Most of the northeastward-pointing WAFs converge around 20°S. The upper-level background mean flow is essentially dominated by easterlies to the north of around 20°S during this season. Therefore, Rossby wave activity originating at midlatitudes being evanescent in this region is reasonable according to the linear theory of Rossby waves [e.g., *Hoskins and Ambrizzi,* 1993].

To emphasize effects of the midlatitude wave propagation on the tropical wave development, we next examine evolution of vertically averaged WAF and eddy kinetic energy (EKE) in a similar way to *Danielson et al.* [2006]. EKE is computed from the composited zonal and meridional wind perturbations. The vertical averaging is performed over the entire troposphere from 1000 to 100 hPa. The vertically averaged values of them well reflect not only the wave activity in the upper level but also that in the low level. These are displayed in Figure 7 at the same timing with Figure 6. From day −4 through day 0, large WAF vectors and increased EKE extend northeastward over the Indian Ocean. The WAF vectors indicate a clear northeastward propagation of wave energy across the subtropical and tropical Indian Ocean. At day −4, the northeastward pointing WAF vectors originate in the SWIO ridge to the east of the South African TTT-like trough (Figure 3b), suggesting that this transient ridge is an energy source for the initial setup of the tropical wave train through the wave energy propagation. From day −2 through day 0, the northeastward WAFs and EKE are further increased over the tropics, which is well synchronous with the northeastward amplification of the low-level tropical waves (Figures 3c and 3d). The strong WAFs emanate from the amplified TTT-like trough over the SWIO at day 0, suggesting that this trough acts as a significant wave energy source for the tropical wave amplification toward the eastern Indian Ocean. It should be noted that we also examined the WAF behavior at 850 hPa (not shown), and the results are similar to that obtained by the analysis based on the vertically averaged values over the SWIO.

We next consider physical processes contributing to the development of troughs and ridges over the SWIO for which EKE may be regarded as an energy source for tropical wave train formation and amplification. *Ray and Zhang* [2010] examined the barotropic energy conversion from the mean flow to disturbances using

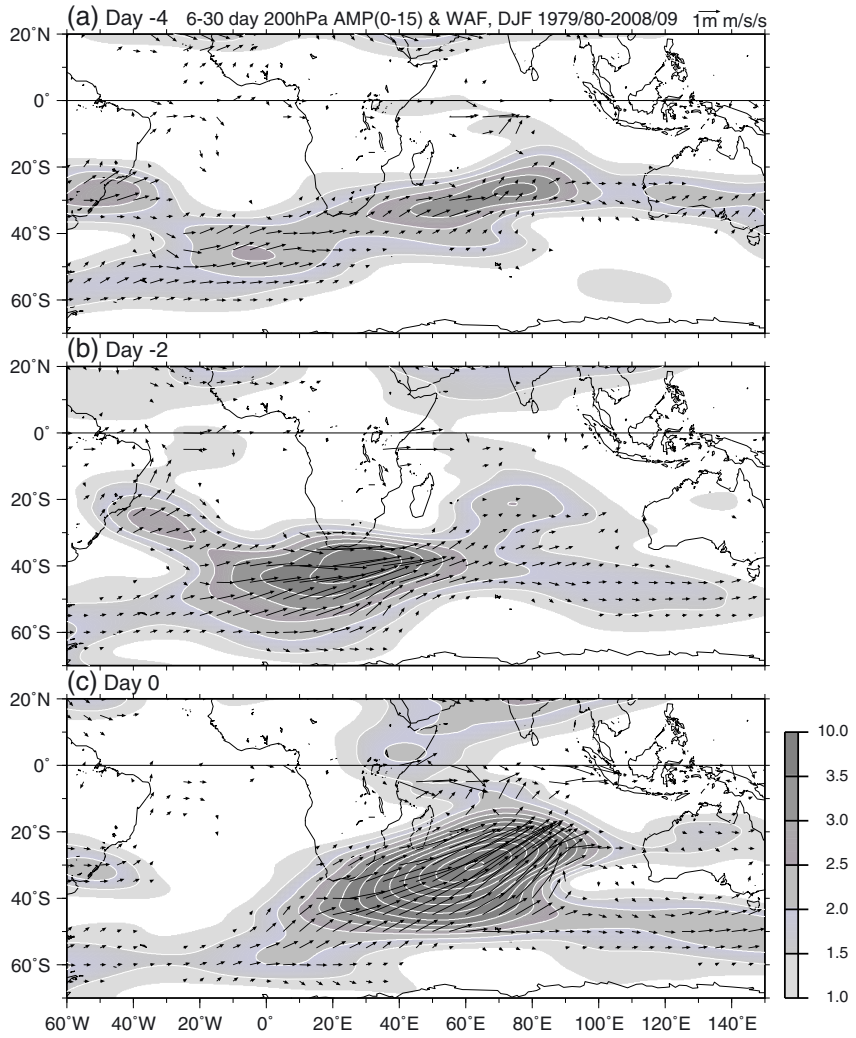

Figure 6. Wave activity flux (WAF) vectors ($m^2\ s^{-2}$) at 200 hPa and amplitude of the waves retaining zonal wave numbers 0–15 of composite 6–30 day meridional wind at 200 hPa on days −4, −2, and 0. Shading shows the amplitude values greater than 1.0 m s^{-1} d^{-1}. Contour interval is 0.5 m s^{-1}.

the formulation derived by *Simmons et al.* [1983] to determine the source of energy for the development of extratropical disturbances affecting the tropics. We adopted an approach similar to that of *Cai and Mak* [1990] and *Deng and Mak* [2006], which apply both barotropic and baroclinic conversion between transient eddies and the mean flow in an eddy kinetic energy tendency equation. The barotropic energy conversion term (BT) they derived is an approximation involving stretching and shearing of the deformation field of the mean flow. Here **E** and **D** are the extended Eliassen-Palm flux of eddies and stretching and shearling deformation field of the mean flow, respectively. They are defined as

$$\mathrm{BT} = \mathbf{E} \cdot \mathbf{D} \tag{1}$$

$$\mathbf{E} = \left[\frac{1}{2}(v'^2 - u'^2), -u'v'\right] \tag{2}$$

$$\mathbf{D} = \left[\frac{\partial \bar{u}}{\partial x} - \frac{\partial \bar{v}}{\partial y}, \frac{\partial \bar{v}}{\partial x} + \frac{\partial \bar{u}}{\partial y}\right] \tag{3}$$

where u' and v' are eddy zonal and meridional winds, and $\bar{u}$ and $\bar{v}$ represent climatological mean zonal and meridional wind.

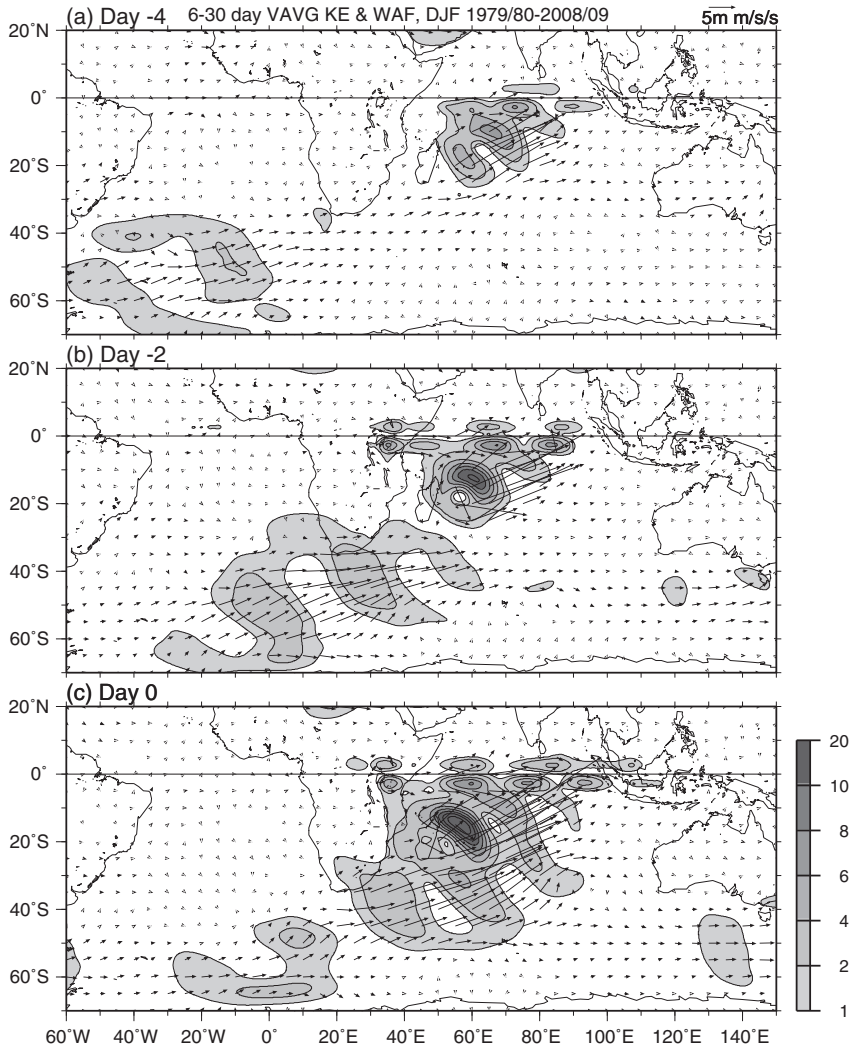

Figure 7. Vertically averaged WAF vectors and eddy kinetic energy (EKE) on days −4, −2, and 0. Shading shows the EKE value greater than 1.0 $m^2\ s^{-2}$. Contour interval is 0.5 $m^2\ s^{-2}$.

The baroclinic conversion term (BC) represents the conversion from the eddy available potential energy to the eddy kinetic energy. This term can be written as

$$\mathrm{BC} = -\frac{R}{p}\omega' T' \tag{4}$$

where ω' is eddy pressure velocity, T' is eddy temperature, p is pressure, and R is the gas constant.

Distribution of the barotropic and baroclinic conversion terms (BT and BC) at day −5 and day −1 are presented in Figures 8 and 9. Day −5 and day 0 are just 1 day prior to the initial development and further amplification of the tropical wave train (day −4 and day −1), respectively. A positive (negative) value indicates an increasing (decreasing) EKE tendency. These terms are computed from the vertically averaged composite eddy quantities so that their relative contribution to the growth of low-level troughs and ridges over the SWIO, which involve upper-level wave propagation, can be compared. In order to easily capture the baroclinic development of the waves originated in the midlatitudes, composite wave patterns in both the lower and upper troposphere are given in Figure 10.

We begin by describing the main features of the BT and BC terms in the southern midlatitudes and subtropical SWIO. BT is predominantly negative in the southern midlatitudes to the south of South Africa and SWIO at both day −5 and day −1 (Figures 8b and 9b). Similar negative BT regions also occur at 850 hPa (data not shown). These regions suggest that the barotropic process tends to dampen the midlatitude-subtropical

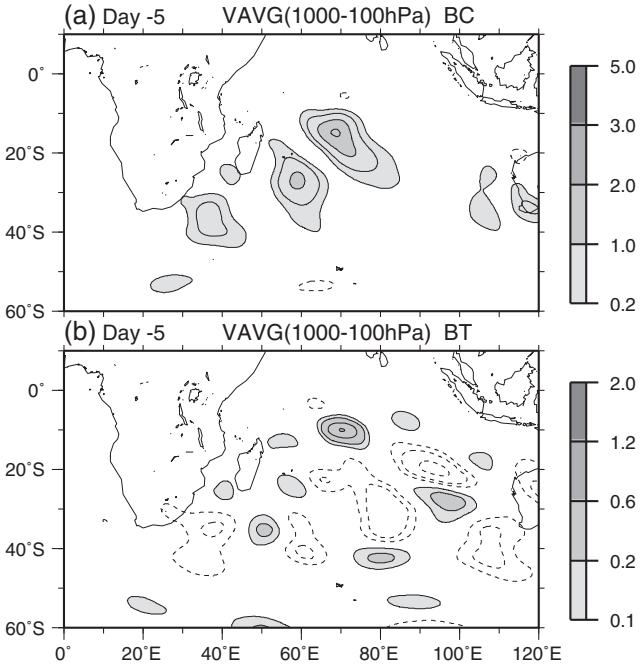

Figure 8. (a) Vertically averaged baroclinic conversion (BC) term on day −5. Values greater than 0.2 ($m^2\ s^{-2}$) d^{-1} are shaded. Contour interval is 0.5. Contours for −0.2 and 0.2 are also plotted. (b) Vertically averaged barotropic conversion (BT) term on day −5. Values greater than 0.1 ($m^2\ s^{-2}$) d^{-1} are shaded. Contour interval is 0.2. Contours for −0.1 and 0.1 are also plotted.

troughs and ridges over the South Africa-SWIO. While positive BC centers are almost in line (Figures 8a and 9a) along the low-level wave train axis (Figures 3b and 3d). At day −5, two BC centers are located in the subtropics and midlatitudes to the southeast of South Africa and the southeast of Madagascar, suggesting that the baroclinic process is a major energy source for the growth of the South African TTT-like trough-SWIO ridge couplet (Figure 3b). At day −1, two positive BC centers occur (Figure 9a) at the eastern and western flank of the TTT-like trough over the SWIO (Figure 3d). Hence, this TTT-like trough also grows primarily due to the baroclinic process. The western BC center lies along the anomalous southerly flow of the trough, and the eastern BC center is located along the anomalous northerly flow of the TTT-like trough and convective band. Therefore, diabatic processes associated with this convective band may be important contributors to the generation of eddy potential energy, which is finally converted to EKE through baroclinic conversion. Composite patterns of the 200 and 850 hPa stream function anomalies from day −4 through day 2 exhibit a baroclinic structure of the waves over the SWIO (Figure 10). At day −4 and day 0, the low-level trough (ridge) axes tend to be located at the northeast of the upper-level trough (ridge) centers over the SWIO, suggesting that baroclinic wave amplification occurs associated with the enhanced BC (Figures 8a and 9a).

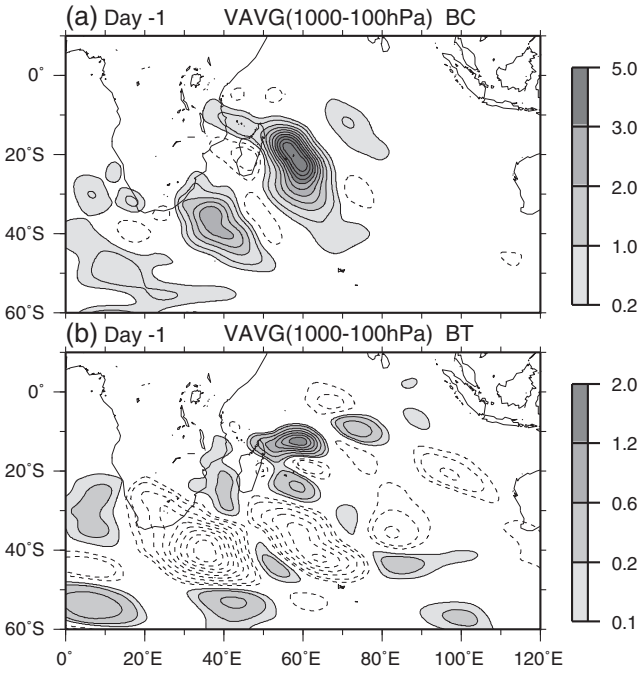

Figure 9. Same as Figure 8 except for day −1.

Although the eddy energetic process in the tropics is not the main focus of this section, several interesting features of the BT and BC terms associated with tropical waves are noted in addition to those already described. As shown in Figures 8b and 9b, regions of positive BT lie along the low-level tropical wave train axis. The BT distribution at 850 hPa also shows similar features (data not shown). This condition prevails throughout the analysis period (data not shown), suggesting that barotropic conversion is a major contributor to the maintenance of the tropical wave train. The BT maxima are almost coincident with the positive meridional shear at the south side of the mean monsoon westerly flow core [as in FY13]. Also, the BT term is dominated by the $-u'v'\partial\overline{u}/\partial y$ term. Therefore, the mean westerly monsoon flow creates favorable conditions for the growth of tropical waves. The baroclinic conversion contributes to the local growth of waves.

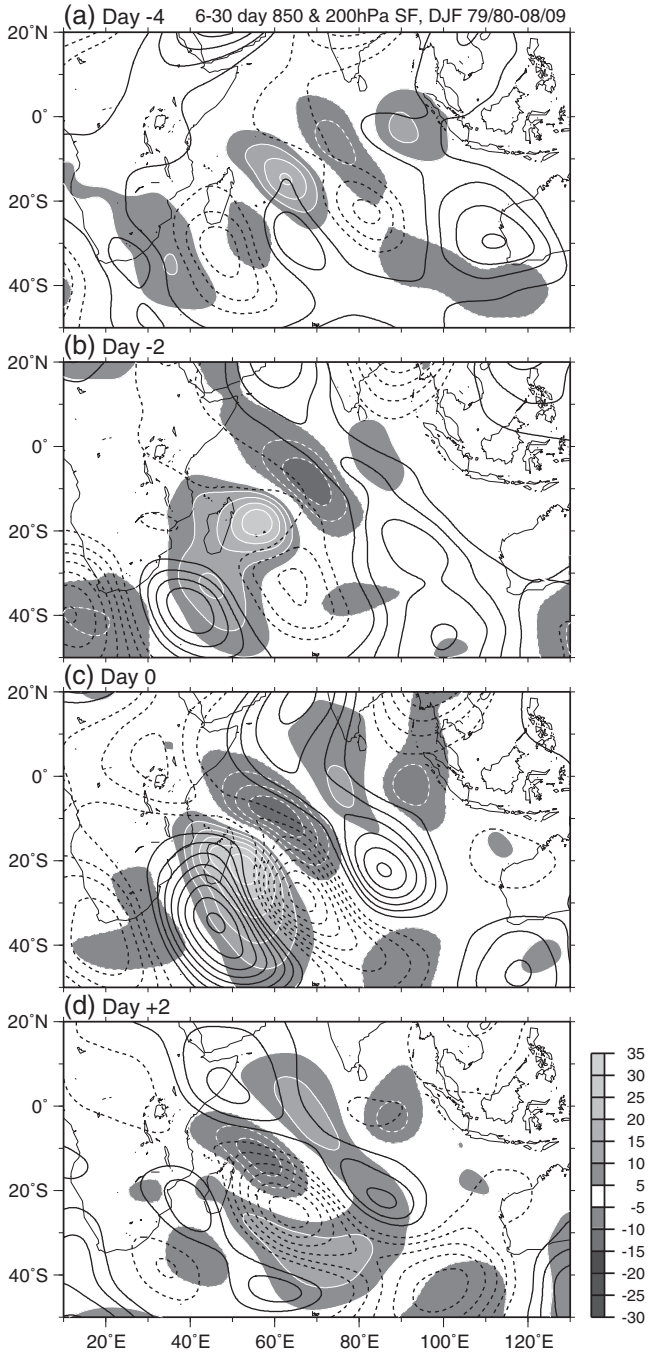

Figure 10. Lagged composites of 6–30 day filtered 200 and 850 hPa stream function anomalies from day −4 through day +2 based on the PC1 index. Shades with white contours represent the 850 hPa anomalies and black contours represent the 200 hPa anomalies. Contour interval is 5.0×10^{-5} s^{-1}. Solid (dashed) contours indicate positive (negative) values.

The maximum BC centered in the tropics (near 70°E, 15°S) at day −5 coincides well with the tropical trough, coupled with convection occurring from day −6 to day −4 (Figures 3a and 3b), suggesting that diabatic processes associated with convection produce baroclinic conversion at the trough.

The diagnostics of wave activity and the simple energetics analysis confirm that the development of the trough and ridge over the SWIO induces the initial formation and further amplification of the tropical wave train. The baroclinic development of the trough and ridge over the SWIO occurs through midlatitude wave propagation. The strong WAFs subsequently emanate from the developed SWIO trough and ridge toward the tropical Indian Ocean, and the EKE along the tropical wave train is enhanced.

5. Summary and Discussion

Statistical analyses were performed to detect the relationship between submonthly scale tropical wave disturbances in the lower troposphere and midlatitude wave propagation over the Indian Ocean. The midlatitude wave propagation toward the subtropics induces the growth of the trough and ridge over the SWIO, and then the amplified trough and ridge act as an energy source for further northeastward development of the tropical waves through a Rossby wave energy dispersion process.

The EEOF analysis identified the tropical wave modes as the two leading EEOFs, which are a quadrature pair indicative of a southwestward propagating signal. The composite analysis based on the first mode time series revealed that tropical waves develop associated with midlatitude waves propagating from the South Atlantic toward the SWIO. Tropical waves form a southwest-northeast-oriented wave train across the tropical Indian Ocean. They propagate westward and southwestward from the equatorial eastern Indian Ocean into the SWIO. The midlatitude wave train progresses eastward and northeastward from the South Atlantic toward the SWIO and establishes the tropical wave train. As a trough-ridge couplet constituting the midlatitude wave train approaches the southern African-SWIO region, formation of the tropical wave train is initiated. Subsequently, the trough of the couplet moves farther northeastward and merges with the tropical trough over the SWIO. This SWIO trough develops with a meridionally elongated convective band and leads to northeastward-eastward amplification of the tropical wave train. This SWIO trough bears a resemblance to a TTT. The early development and further amplification of the tropical wave train is induced by Rossby wave energy dispersion originating in the southern African-SWIO trough-ridge couplet and SWIO trough. Low-level trough and ridge development in the southern African-SWIO region is induced by the upper-level midlatitude wave propagation through a baroclinic process. As the upper-level waves propagate northeastward from the South Atlantic into the subtropical Indian Ocean, they strengthen through wave energy dispersion and form a southwest-northeast-oriented wave train. Growth of the low-level trough occurs northeastward ahead of the upper-level trough as part of the midlatitude wave train located over the southern African-SWIO region. Series of physical processes are emphasized by the wave activity diagnostics and simple energetics analysis. Results of the analysis suggest that midlatitude wave propagation toward the SWIO is one of the fundamental mechanisms behind the development of the tropical wave train.

The mechanism for the extratropical influence on the development of the tropical waves over the Indian Ocean is somewhat analogous to that observed in the Pacific region [e.g., *Kiladis,* 1998; *Straub and Kiladis,* 2003], in terms of equatorward propagation of upper-level waves from the extratropics. The upper-level waves associated with the excitation of topical convective waves over the Pacific tend to propagate into the deep tropics. They are directly linked to the enhancement of the low-level convective waves. *Kiladis* [1998] demonstrated that the upper-level waves propagating into the eastern equatorial Pacific from the Asian subtropical jet excite equatorial Rossby waves in the ITCZ. On the other hand, *Straub and Kiladis* [2003] illustrated that the upper-level waves propagating into the western equatorial Pacific from the Australian subtropical jet force equatorial Kelvin waves in the western Pacific ITCZ. However, the current results do not show direct excitation of the low-level tropical waves by the upper-level waves. As depicted in the previous sections, the upper-level waves associated with the low-level wave development over the tropical Indian Ocean marginally pass through the off-equatorial tropics. The low-level tropical waves are enhanced due to the low-level wave energy dispersion originating in the SWIO trough and ridge which are amplified by the upper-level wave propagation.

As mentioned previously, the South African and SWIO TTT-like troughs are established associated with the tropical wave development. In particular, the SWIO TTT-like trough couples with the pronounced convective band. This situation corresponds well to an enhancement of convection along the South Indian Convergence Zone (SICZ) [*Cook*, 2000; *Ninomiya*, 2008]. Several previous studies have recognized that the SICZ is one of the preferred locations for the development of TTTs [*Fauchereau et al.,* 2009; *Manhique et al.,* 2009; *Pohl et al.,* 2009; *Cretat et al.,* 2012; *Hart et al.,* 2010; *Vigaud et al.,* 2012]. Hence, one may reasonably suppose that the SWIO TTT-like trough seen in the composites is a form of TTT along the SICZ, which raises an intriguing question as to the relationship between the tropical waves, the TTTs generally seen in the southern African-SWIO region and the SH midlatitude waves. Previous studies on TTTs clarified that TTT formation is essentially induced by SH midlatitude wave propagation from the South Atlantic toward the SWIO. While these studies did not indicate a strong linkage between TTTs and tropical wave activity, it implies that not all TTT events are related to tropical wave train development. However, that does not

preclude the possibility of a close relationship between tropical wave development and TTT formation. *Lyons* [1991] and *Pohl et al.* [2009] noted a linkage between TTT and tropical wave disturbances over the Indian Ocean. Therefore, we can expect that a particular type of TTT event is responsible for the development of tropical wave trains. The importance of TTTs for the development of tropical waves over the tropical Indian Ocean will be investigated further as a natural extension of this study. An identification of transient TTT events as demonstrated by *Ratna et al.* [2012] is necessary to conduct this further work.

Multiscale interaction between the submonthly tropical waves and various-scale disturbances such as MJO tropical cyclones might also be considered as a subject for a future study. Although previous works concerned the interaction between submonthly tropical convective disturbances and the MJO, they mainly focused on interactive phenomena such as those over the Pacific [e.g., *Meehl et al.*, 1996; *Matthews and Kiladis,* 1999]. *Vincent et al.* [1998] showed that both submonthly and MJO-scale convective activity are aligned with the Indian Ocean ITCZ and found an interannual relationship between these activities. However, interactions between the submonthly wave disturbances and the MJO in this region have not been well clarified. FY13 suggested that the mean westerly monsoon flow constituting the seasonal (DJF) mean state provides favorable background conditions for the propagation and maintenance of submonthly scale waves. The westerly monsoon flow changes substantially on low-frequency intraseasonal timescales as a result of the MJO. Studies are needed on how MJO-scale low-frequency changes to the westerly monsoon flow affect the submonthly wave activity. The dynamical role of the MJO in the development of submonthly scale waves along the Indian Ocean ITCZ will also be examined in the future.

Acknowledgments
We appreciate the comments of three anonymous reviewers, which helped to improve an earlier version of the paper. We also thank Kotaro Takaya for suggestions for application of wave activity diagnostics.

References

Cai, M., and M. Mak (1990), On the basic dynamics of regional cyclogenesis, *J. Atmos. Sci.*, *47*, 1417–1442.
Chang, E. K. M., and D. B. Yu (1999), Characteristics of wave packets in the upper troposphere, Part I: Northern Hemisphere winter, *J. Atmos. Sci.*, *56*, 1708–1728.
Chu, P.-S. (1988), Extratropical forcing and the burst of equatorial westerlies in the western Pacific, *J. Meteorol. Soc. Jpn.*, *66*, 549–563.
Compo, G. P., G. N. Kiladis, and P. J. Webster (1999), The horizontal and vertical structure of east Asian winter monsoon pressure surges, *Q. J. R. Meteorol. Soc.*, *125*, 29–54.
Cook, K. (2000), The South Indian Convergence Zone and interannual rainfall variability over southern Africa, *J. Climate*, *21*, 3789–3804.
Cretat, J., Y. Richard, B. Pohl, M. Rouault, C. J. C. Reason, and N. Fauchereau (2012), Recurrent daily rainfall patterns over South Africa and associated dynamics during the core of the austral summer, *Int. J. Climatol.*, *32*, 161–320, doi:10.1002/joc.2266.
Danielson, R. E., J. R. Gyakum, and D. N. Straub (2006), A case study of downstream baroclinic development over the north Pacific Ocean. Part II: Diagnoses of eddy energy and wave activity, *Mon. Weather Rev.*, *134*, 1549–1567.
Davidson, N. E., K. J. Tory, M. J. Reader, and W. L. Drosdowsky (2007), Extratropical–tropical interaction during onset of the Australian monsoon: Reanalysis diagnostics and idealized dry simulations, *J. Atmos. Sci.*, *64*, 3475–3498.
de Laat, A. T. J., and J. Lelieveld (2002), Interannual variability of the Indian winter monsoon circulation and consequences for pollution levels, *107*, *4739*, doi:10.1029/2001JD001483.
Deng, Y., and M. Mak (2006), Nature of the differences in the intraseasonal variability of the Pacific and Atlantic storm tracks: A diagnostic study, *J. Atmos. Sci.*, *63*, 2602–2615.
Fauchereau, N., B. Pohl, C. J. C. Reason, M. Rouault, and Y. Richard (2009), Recurrent daily OLR patterns in the Southern Africa/Southwest Indian Ocean region, implications for South African rainfall and teleconnections, *Clim. Dyn.*, *32*, 575–591.
Fukutomi, Y., and T. Yasunari (2005), Southerly surges on submonthly time scales over the eastern Indian Ocean during the Southern Hemisphere winter, *Mon. Weather Rev.*, *133*, 1637–1654.
Fukutomi, Y., and T. Yasunari (2009), Cross-equatorial influences of submonthly scale southerly surges over the eastern Indian Ocean during the Southern Hemisphere winter, *J. Geophys. Res.*, *133*, 1637–1654, doi:10.1029/2008JD011441.
Fukutomi, Y., and T. Yasunari (2013), Structure and characteristics of submonthly-scale waves along the Indian Ocean ITCZ, *Clim. Dyn.*, *40*, 1819–1839, doi:10.1007/s00382-012-1417-x.
Hart, N. C. G., C. J. C. Reason, and N. Fauchereau (2010), Tropical–extratropical interactions over Southern Africa: Three cases of heavy summer season rainfall, *Mon. Weather Rev.*, *138*, 2608–2623.
Hoskins, B. J., and T. Ambrizzi (1993), Rossby wave propagation on a longitudinally varying flow, *J. Atmos. Sci.*, *50*, 1661–1671.
Hsu, H.-H., and S.-H. Lin (1992), Global teleconnections in the 250-mb streamfunction field during the Northern Hemisphere winter, *Mon. Weather Rev.*, *120*, 1169–1190.
Kaylor, R. E. (1977), *Filtering and Decimation of Digital Time Series*, Tech Note BN 850, Institute of Physical Science and Technology, Univ. of Maryland, College Park.
Kiladis, G. N., G. A. Meehl, and K. M. Weickmann (1994), Large-scale circulation associated with westerly wind bursts and deep convection over the western equatorial Pacific, *J. Geophys. Res.*, *99*, 18,527–18,544.
Kiladis, G. N. (1998), Observations of Rossby waves linked to convection over the eastern tropical Pacific, *J. Atmos. Sci.*, *55*, 321–339.
Krishnamurti, T. N, B. Jha, P. J. Rasch, and V. Ramanathan (1997), A high resolution global reanalysis highlighting the winter monsoon. Part II: Transients and passive tracer transports, *Meteorol. Atmos. Phys.*, *64*, 151–171.
Lau, K.-H., and N.-C. Lau (1990), Observed structure and propagation characteristics of tropical summertime synoptic scale disturbances, *Mon. Weather Rev.*, *118*, 1888–1913.
Love, G. (1985), Cross-equatorial influence of winter hemisphere subtropical cold surges, *Mon. Weather Rev.*, *113*, 1487–1498.
Lyons, S. W. (1991), Origins of convective variability over equatorial southern Africa during austral summer, *J. Climate*, *4*, 23–39.
Maloney, E. D., and M. J. Dickinson (2003), The intraseasonal oscillation and the energetics of summertime tropical western north Pacific synoptic-scale disturbances, *J. Atmos. Sci.*, *60*, 2153–2168.

Manhique, A. J., C. J. C. Reason, L. Rydberg, and N. Fauchereau (2009), ENSO and Indian Ocean sea surface temperatures and their relationships with tropical temperate troughs over Mozambique and the Southwest Indian Ocean, *Int. J. Climatol.*, *31*, 1–13, doi:10.1002/joc.2050.

Matthews, A. J., and G. N. Kiladis (1999), Interactions between ENSO, transient circulation, and tropical convection over the Pacific, *J. Climate*, *12*, 3062–3086.

Meehl, G. A., G. N. Kiladis, K. M. Weickmann, M. Wheeler, D. S. Gutzler, and G. P. Compo (1996), Modulation of equatorial subseasonal convective episodes by tropical-extratropical interaction in the Indian and Pacific Ocean regions, *J. Geophys. Res.*, *101*, 15,033–15,049.

Ninomiya, K. (2008), Similarities and differences among the South Indian Ocean Convergence Zone, North American Convergence Zone, and other subtropical convergence zones simulated using an AGCM, *J. Meteorol. Soc. Jpn*, *86*, 141–165.

Onogi, K., et al. (2005), JRA-25: Japanese 25-year re-analysis–Progress and status, *Q. J. R. Meteorol. Soc.*, *131*, 3259–3268.

Onogi, K., et al. (2007), The JRA-25 analysis, *J. Meteorol. Soc. Jpn.*, *85*, 369–432.

Pohl, B., N. Fauchereau, Y. Richard, M. Rouault, and C. J. C. Reason (2009), Interactions between synoptic, intraseasonal and interannual convective variability over Southern Africa, *Clim. Dyn.*, *33*, 1033–1050.

Ramanathan, V., et al. (2001), Indian Ocean Experiment: An integrated analysis of climate forcing and effects of the great Indo-Asian haze, *J. Geophys. Res.*, *106*, 28,371–28,398.

Ratna, S. B., S. Behera, J. V. Ratnam, K. Takahashi, and T. Yamagata (2012), An index for topical temperate troughs over southern Africa, *Clim. Dyn.*, *41*, 421–441, doi:10.1007/s00382-012-1540-8.

Ray, P., and C. Zhang (2010), A case study of the mechanisms of extratropical influence on the initiation of the Madden–Julian Oscillation, *J. Atmos. Sci.*, *67*, 515–528.

Schrage, J. M., C. A. Clayson, and B. Strahl (2001), Statistical properties of episodes of enhanced 2–3-day convection in the Indian and Pacific oceans, *J. Climate*, *14*, 3482–3494.

Seager, R., N. Naik, M. Cane, N. Harnik, M. Ting, and Y. Kushnir (2010), Adjustment of the atmospheric circulation to tropical Pacific SST anomalies: Variability of transient eddy propagation in the Pacific–North America sector, *Q. J. R. Meteorol. Soc.*, *136*, 277–296.

Simmons, A. J., J. M. Wallace, and G. W. Branstator (1983), Barotropic wave propagation and instability and atmospheric teleconnection patterns, *J. Atmos. Sci.*, *40*, 1363–1392.

Slingo, J. M. (1998), Extratropical forcing of tropical in a northern winter simulation with the UGAMP GCM, *Q. J. R. Meteorol. Soc.*, *124*, 27–51.

Straub, H. H., and G. N. Kiladis (2003), Extratropical forcing of convectively coupled Kelvin waves during austral winter, *J. Atmos. Sci.*, *60*, 526–543.

Takaya, K., and H. Nakamura (1997), A formulation of a wave-activity flux for stationary Rossby waves on a zonally varying basic flow, *Geophys. Res. Lett.*, *24*, 2985–2988.

Takaya, K., and H. Nakamura (2001), A formulation of a phase-independent wave-activity flux for stationary and migratory quasi-geostrophic eddies on a zonally varying basic flow, *J. Atmos. Sci.*, *58*, 608–627.

Vera, C. S., P. K. Vigliarolo, and E. H. Berbery (2002), Cold season synoptic-scale waves over subtropical South America, *Mon. Weather Rev.*, *130*, 684–699.

Verver, G. H. L., D. R. Sikka, J. M. Lobert, G. Stossmeister, and M. Zachariasse (2001), Overview of the meteorological conditions and atmospheric transport processes during INDOEX 1999, *J. Geophys. Res.*, *106*, 28,399–28,413.

Vigaud, N., B. Pohl, and J. Cretat (2012), Tropical-temperate interactions over southern Africa simulated by a regional climate model, *Clim. Dyn.*, *39*, 2895–2916, doi:10.1007/s00382-012-1214-3.

Vincent, D. G., A. Fink, J. M. Schrage, and P. Speth (1998), High- and low-frequency intraseasonal variance of OLR on annual and ENSO timescales, *J. Climate*, *11*, 968–986.

Yu, L., and M. M. Rienecker (1998), Evidence of an extratropical influence during the onset of 1997–1998 El Niño, *Geophys. Res. Lett.*, *25*, 3537–3540.